The
University
Of
Sheffield.

This is a repository copy of *A stem spacing-based non-dimensional model for predicting longitudinal dispersion in low-density emergent vegetation*.

White Rose Research Online URL for this paper:
http://eprints.whiterose.ac.uk/138088/

Version: Published Version

Article:

White Rose
university consortium
Universities of Leeds, Sheffield & York

eprints@whiterose.ac.uk
https://eprints.whiterose.ac.uk/

CrossMark

A stem spacing-based non-dimensional model for predicting longitudinal dispersion in low-density emergent vegetation

F. Sonnenwald[1] · V. Stovin[1] · I. Guymer[1]

Abstract

Predicting how pollutants disperse in vegetation is necessary to protect natural watercourses. This can be done using the one-dimensional advection dispersion equation, which requires estimates of longitudinal dispersion coefficients in vegetation. Dye tracing was used to obtain longitudinal dispersion coefficients in emergent artificial vegetation of different densities and stem diameters. Based on these results, a simple non-dimensional model, depending on velocity and stem spacing, was developed to predict the longitudinal dispersion coefficient in uniform emergent vegetation at low densities (solid volume fractions < 0.1). Predictions of the longitudinal dispersion coefficient from this simple model were compared with predictions from a more complex expression for a range of experimental data, including real vegetation. The simple model was found to predict correct order of magnitude dispersion coefficients and to perform as well as the more complex expression. The simple model requires fewer parameters and provides a robust engineering approximation.

Introduction

The fate of pollutants in stormwater is of interest to protect natural watercourses. To predict how pollutants will disperse in these systems, one-dimensional (1D) modelling based on the advection–dispersion equation (ADE) is commonly used (DHI 2009). The 1D ADE is typically given as:

$$\frac{\partial C}{\partial t} + U\frac{\partial C}{\partial x} = D_x\left(\frac{\partial^2 C}{\partial x^2}\right) \qquad (1)$$

where C is cross-sectional mean concentration, t is time, U is mean longitudinal velocity, x is the longitudinal coordinate, and D_x is the longitudinal dispersion coefficient (Fischer et al. 1979). U and D_x are required to use the equation predictively.

Natural watercourses often contain vegetation (O'Hare 2015). Furthermore, prior to entering natural watercourses, stormwater is often treated within vegetated sustainable drainage systems (SuDS) to reduce the quantity of pollutants

in surface runoff (Woods-Ballard et al. 2015). Applying the 1D ADE to predict pollutant transport therefore requires estimates of longitudinal dispersion coefficient (D_x) within vegetation. While velocities can be estimated from simple hydraulics or numerical models, reliable estimation of the longitudinal dispersion coefficient based on vegetation characteristics is often problematic (Sonnenwald et al. 2017). This paper investigates the prediction of the longitudinal dispersion coefficient in uniform emergent vegetation at low densities. It presents results from new laboratory measurements of longitudinal dispersion and compares new and existing predictors of longitudinal dispersion coefficient to measured values.

Predicting D_x in vegetation

Vegetation can be characterised by stem diameter d, solid volume fraction ϕ, frontal facing area a (the vegetation area perpendicular to the direction of flow per unit volume), and mean stem edge-to-edge spacing s. Assuming vegetation may be represented as an array of vertical cylinders, these parameters are related by $\phi = ad\pi 4^{-1}$. Tanino and Nepf (2008) provided:

✉ F. Sonnenwald
    f.sonnenwald@sheffield.ac.uk

1   Department of Civil and Structural Engineering, University
    of Sheffield, Sheffield, UK

$$s \approx d\sqrt{\frac{1+2\phi}{4\phi} - \sqrt{\pi}\sqrt{\frac{1-2\phi}{4\phi}}\frac{\left[1 - \text{erf}\left(\sqrt{4\phi/1-2\phi}\right)\right]}{\exp\left(-4\phi/(1-2\phi)\right)}} - 1$$

(2)

to estimate s based on stem diameter and solid volume fraction for a random array of cylinders. As there are multiple stem spacing values for a given vegetation configuration, stem spacing may also be characterised by s_{50}, the median stem spacing. While $s \approx s_{50}$ when vegetation stem spacing is uniformly or normally distributed, this is not the case when the distribution of stem spacing is asymmetric (e.g. many small stems but few large ones).

Tanino (2012), in a review of mixing in vegetation, suggested that there are primarily three mixing mechanisms contributing to longitudinal dispersion within emergent vegetation: turbulent diffusion; secondary wake dispersion; and vortex trapping. Turbulent diffusion within vegetation is the result of instantaneous velocity fluctuations caused by eddies generated by stems. Secondary wake dispersion is caused by velocity-field heterogeneity resulting in different travel times for particles (differential advection). Vortex trapping is caused by the temporary entrainment of particles in vortices behind stems.

Of these three processes, only secondary wake dispersion contributes significantly to longitudinal dispersion at low densities ($\phi < 0.1$). Turbulent diffusion is the primary transverse mixing mechanism at low densities (Tanino and Nepf 2008). However, as total transverse dispersion is typically an order of magnitude lower than total longitudinal dispersion (Sonnenwald et al. 2017), it does not make a significant contribution to longitudinal dispersion. Similarly, dispersion due to vortex trapping is typically much lower than secondary wake dispersion at low densities (White and Nepf 2003). Therefore, secondary wake dispersion should provide a reasonable approximation of total longitudinal dispersion within vegetation at low densities.

White and Nepf (2003) explained that secondary wake dispersion is the sum of two processes: a wake contribution and a gap contribution. The former is caused by reductions in velocity behind stems and the latter caused by increases in velocity between stems. For low densities, the gap contribution is much lower than the wake contribution, and hence, White and Nepf (2003) suggested that longitudinal dispersion in vegetation may be estimated utilising:

$$D_x = 2\sigma_u^{*2}s^*\sqrt{\frac{Sc_t}{Sc_t + 1}}Ud$$

(3)

where σ_u^{*2} is the variance of the longitudinal velocity field normalised by mean longitudinal velocity squared, $s^* = (s + d)d^{-1}$, and Sc_t is the turbulent Schmidt number. The

variance term represents the level of velocity perturbation caused by stems throughout the velocity field. These parameters can be non-trivial to estimate for a specific vegetation, and so Lightbody and Nepf (2006) combined several parameter estimates and presented:

$$D_x = \frac{1}{2}C_D^{3/2}Ud$$

(4)

where C_D is the drag coefficient.

Calculating C_D in vegetation depends either on having very precise measurements of the energy gradient or on having a direct force sensor (Tinoco and Cowen 2013). Both methods are difficult to apply in practice, and as such, it is often preferable to use an estimate of C_D, e.g. $C_D = 1$. C_D may also be estimated based on the Ergun (1952) expression for pressure drop in a packed column as:

$$C_D = 2\left(\frac{6475d + 32}{Re_d} + 17d + 3.2\phi + 0.5\right)$$

(5)

where $Re_d = Ud\nu^{-1}$ is stem Reynolds number and ν is kinematic viscosity (Sonnenwald et al. 2018b).

Comparison of Eq. (4) to experimental data suggested that it provides correct order of magnitude predictions of the longitudinal dispersion coefficient in vegetation when using values of C_D estimated with Eq. (5) (Sonnenwald et al. 2018a). However, Eq. (4) depends on several simplifying assumptions for values of σ_u^{*2} and Sc_t and is insensitive to C_D. A simplified model has previously been developed by Nepf (2012) for predicting the transverse dispersion coefficient in emergent vegetation based on velocity and stem diameter. This paper aims to explore whether a similar approach could be adopted for predicting the longitudinal dispersion coefficient in emergent vegetation.

Previous studies

Several previous experimental studies have investigated the longitudinal dispersion coefficient in emergent vegetation at low density; these studies are summarised in Table 1. The majority of these studies investigated dispersion in real vegetation. As the natural variability of real vegetation does not lend itself to generalisation, additional experiments investigating longitudinal dispersion in artificial emergent vegetation have been carried out by the authors, as described below.

Methodology

A 15-m long, 300-mm-wide recirculating Armfield flume was fitted with uniform artificial emergent vegetation, and dye tracing was conducted. Uniform flow was established

Table 1 Previous studies investigating longitudinal dispersion in uniform emergent vegetation

Description	d (mm)	ϕ	s (mm)[a]	U (mm s^{-1})	References
Mixed real species	1–10	0.002–0.022	7–26	14–38	Huang et al. (2008)
Artificial random	6	0.010–0.055	8–25	29–74	Nepf et al. (1997)
Carex	10–55	0.002–0.059	70–104	99–232	Shucksmith et al. (2010)
Phragmites australis	3	0.002	28–30	171–242	Shucksmith et al. (2010)
Regular periodic	4	0.005	51.9[b]	7–50	Sonnenwald et al. (2016)
Typha latifolia	10–19	0.013–0.047	29–36	9–29	Sonnenwald et al. (2017)
Artificial random	6	0.010–0.064	7–25	12–97	White and Nepf (2003)

[a]Estimated using Eq. (2)

[b]Known, not estimated, value

at velocities of 7–122 mm s^{-1} by adjusting flume slope and tailgate, and confirmed using point gauges along the length of the flume. Flow depth was set at 150 mm. A diffuser plate was placed directly after the inlet to straighten the flow.

Three cylinder array configurations representing vegetation were examined. These were a regular periodic configuration, a pseudo-random configuration, and a random configuration. The artificial vegetation was constructed by inserting 4-mm-diameter drinking straws or 8-mm-diameter plastic dowels into plastic base plates laid into the bottom of the flume. Two types of base plates were constructed: one with a regular periodic pattern and one with a random pattern. The regular pattern base plate was drilled such that if every hole were filled with drinking straws, the solid volume fraction would be 0.02. However, stems were placed in only 1 out of every 4 holes in a regular pattern, giving $\phi = 0.005$. This allowed for the same number of stems to be repositioned on the regular plates in a new pattern with the stem positions chosen at random, giving the pseudo-random vegetation pattern. The random pattern for the second base plate was chosen so that stems would not touch, but allowed for stems to have a machined face (producing a cylinder segment) that could be placed against the flume walls. These three configurations allow the effects of stem diameter, arrangement, and density to be compared. The vegetation configurations are illustrated in Fig. 1.

The characteristics of the artificial vegetation are given in Table 2. Three different stem spacing measurements are provided: a mean value estimated using Eq. (2), the known mean value, and the median stem spacing. This illustrates how stem spacing measurements can vary depending on configuration. The regular periodic vegetation is an expanded data set from the previous Sonnenwald et al. (2016) study, and hence, comparisons are not made to that previous study.

Rhodamine WT dye tracing was carried out using four mid-channel mid-depth Turner Designs Cyclops 7 fluorometers to record temporal concentration profiles. The four fluorometers formed three 2.5-m test reaches for the 4-mm stems and three 3-m test reaches for the 8-mm stems, giving total experimental lengths of 7.5 m and 9 m, respectively. The
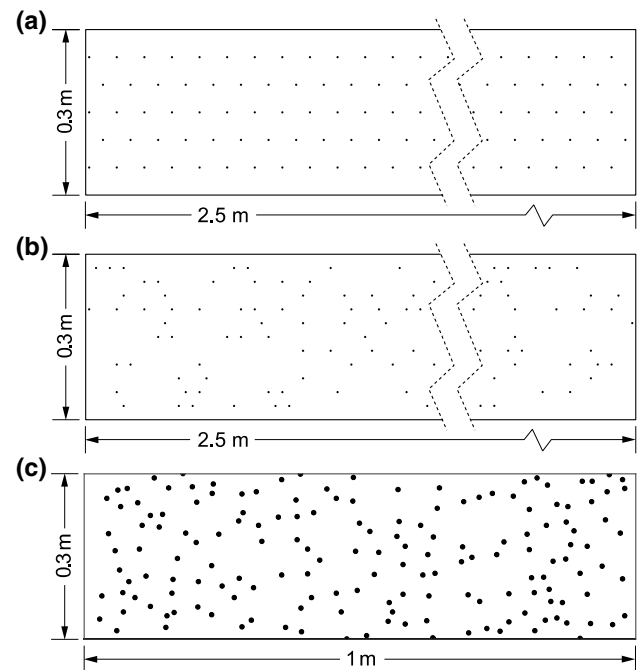

Fig. 1 Vegetation configuration illustrations **a** regular periodic vegetation reach layout with 4-mm stems, the vegetation pattern repeats every 0.05 m, **b** pseudo-random vegetation reach layout with 4-mm stems, the vegetation pattern repeats every 2.5 m, and **c** random vegetation reach layout with 8-mm stems, the vegetation pattern repeats every 1 m

Table 2 Artificial emergent vegetation characterisation

Description	d (mm)	ϕ	Estimated s (mm)[a]	s (mm)[b]	s_{50} (mm)
Regular periodic[c]	4	0.005	24.9	51.9	51.9
Pseudo-random	4	0.005	24.9	29.4	23.9
Random	8	0.027	18.0	22.7	22.3

[a]Estimated mean stem spacing using Eq. (2)

[b]Known mean stem spacing

[c]These data include additional measurements to those presented in Sonnenwald et al. (2016)

first fluorometer was located 4 m downstream of the inlet diffuser plate. The different reach lengths were to accommodate the difference in vegetation pattern repetition. The 4-mm stems covered the full length of the flume. The 8-mm stems covered between 3 m and 14 m from the inlet diffuser plate, with 1 m before and after the first and last fluorometer.

Three injections were carried out at each velocity, giving nine sets of upstream and downstream temporal concentration profiles recorded at 1 Hz. Manual pulse injections were made directly into the inlet pipe of the flume to ensure that the flow was well mixed. Regular periodic vegetation was investigated at target velocities of 7, 10, 13, 17, 20, 30, 40, and 50 mm s^{-1}, pseudo-random vegetation at 7, 10, 13, 17, 20, 30, 40, 50, 60, 90, and 110 mm s^{-1}, and random vegetation at 10, 30, 55, 80, 100, and 120 mm s^{-1}. Photographs of the experimental setup are shown in Fig. 2.

Determining D_x from experimental results

Values of D_x were found using the following routing solution to the 1D ADE,

$$C(x_2, t) = \int_{\tau=-\infty}^{\infty} \frac{C(x_1, t)U}{\sqrt{4\pi D_x \bar{t}}} \exp\left(-\frac{U^2(\bar{t} - t + \tau)^2}{4D_x \bar{t}}\right) d\tau \quad (6)$$

where $C(x_1, t)$ and $C(x_2, t)$ are upstream and downstream concentration profiles, respectively, $\bar{t}$ is travel time, and τ is an integration variable (Fischer et al. 1979). The MATLAB (The MathWorks Inc. 2018) *lsqcurvefit* function was used to minimise the sum of errors squared between the measured and a predicted downstream temporal concentration profile to produce optimised values of D_x and U.
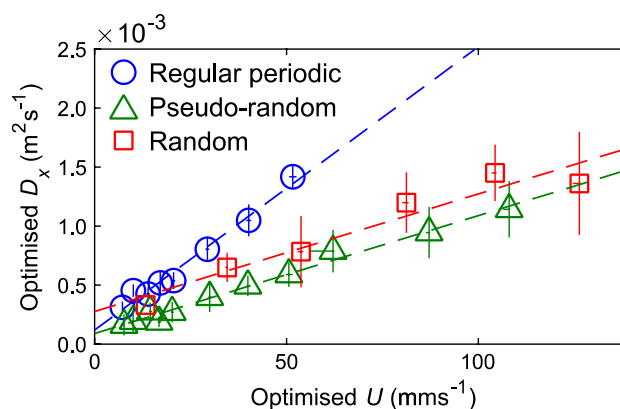

Fig. 3 Optimised longitudinal dispersion coefficient plotted against optimised velocity, dashed lines are best-fit linear trend lines with RMSE = 5.073×10^{-5}, 3.583×10^{-5}, and 1.069×10^{-4} for the regular periodic, pseudo-random, and random vegetation, respectively, vertical and horizontal error bars indicate 95% CIs

Results and discussion

Figure 3 presents mean longitudinal dispersion coefficient as a function of velocity, showing the expected linear trend of increasing D_x with U for all configurations. The near identical slope for the pseudo-random and random vegetation was not expected as the vegetation arrays are visually quite different and have different characteristics, notably different stem diameters.

Figure 4 presents non-dimensional longitudinal dispersion coefficient (with respect to stem diameter) as a function of velocity. For velocities greater than approximately 20 mm s^{-1}, the results confirm the linear dependency on U shown in Fig. 3. However, at velocities < 20 mm s^{-1}, the dependency is not linear. The lower velocities correspond roughly to $Re_d < 100$. Nepf (1999) suggested that turbulent diffusion could be significantly reduced at low velocities, which by definition corresponds with a greatly increased longitudinal dispersion, as observed here. Notably in Fig. 4,
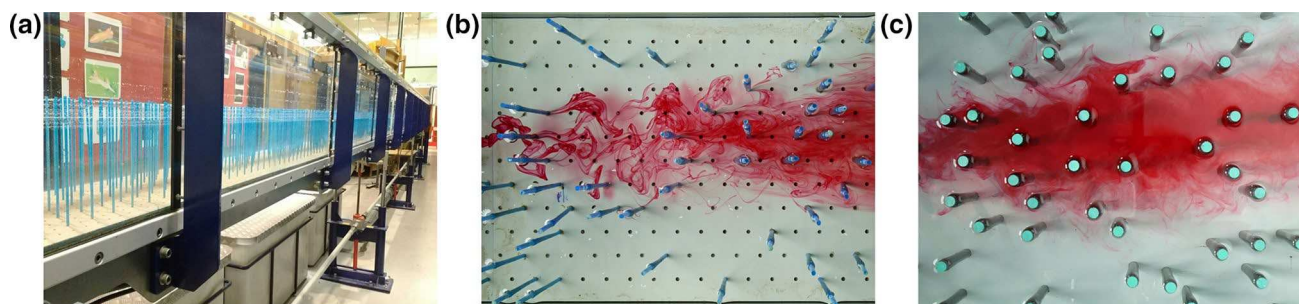

Fig. 2 Photographs of experimental setup, dye is from manual injection to water surface for illustration purpose **a** regular periodic, showing Armfield flume, **b** pseudo-random, snapshot of continuous injection at $U = 7$ mm s^{-1} and **c** random vegetation, snapshot of pulse injection at $U = 11$ mm s^{-1}
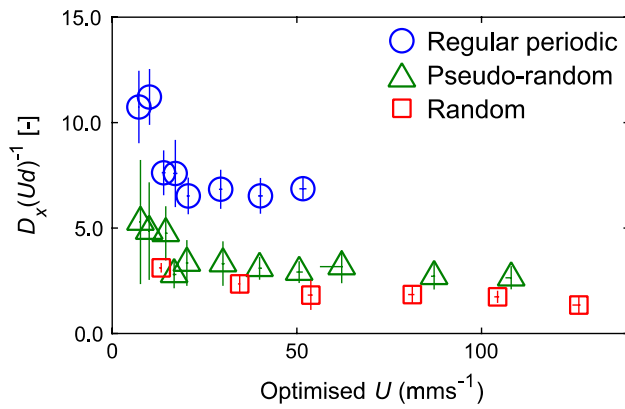
Fig. 4 Non-dimensional longitudinal dispersion coefficient with respect to stem diameter, $D_x(Ud)^{-1}$, plotted against velocity, vertical and horizontal error bars indicate 95% CIs
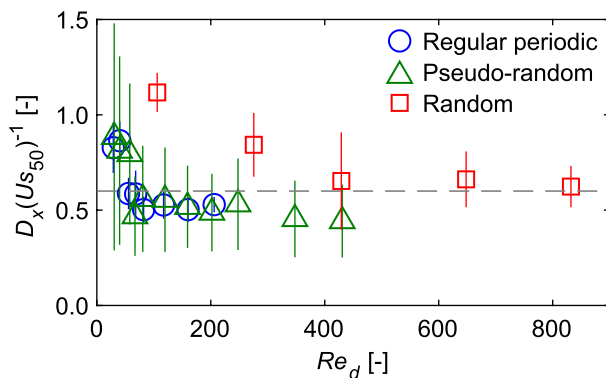

Fig. 5 Non-dimensional longitudinal dispersion coefficient with respect to stem spacing, $D_x(Us_{50})^{-1}$ plotted against stem Reynolds number, the dashed line is Eq. (7), vertical and horizontal error bars indicate 95% CIs

measurements of D_x from all three vegetation configurations do not collapse to a single line, contrary to the relationships suggested by Eqs. (3) and (4), both of which normalise by d. This suggests an alternative scale should be used for normalisation.

Figure 5 shows $D_x(Us_{50})^{-1}$, the non-dimensional longitudinal dispersion coefficient normalised by median stem spacing, plotted with respect to the stem Reynolds number. Stem spacing is used here given that it changes between the regular periodic and pseudo-random vegetation. The random vegetation has slightly higher values of $D_x(Us_{50})^{-1}$ than the regular and pseudo-random vegetation, which behave very similarly. Although there is a significant variation in $D_x(Us_{50})^{-1}$ at $Re_d < 100$, all three types of vegetation have similarly consistent values of $D_x(Us_{50})^{-1}$ at $Re_d \gtrsim 100$. This demonstrates, for the first time, the practicality of normalising longitudinal dispersion coefficient in vegetation by stem spacing. The regular and pseudo-random vegetation have

similar non-dimensional dispersion coefficient values at all Re_d, including $Re_d < 100$, as would be expected for two types of vegetation with the same d and ϕ.

From the results in Fig. 5, a non-dimensional model for longitudinal dispersion based on stem spacing is proposed:

$$D_x = 0.60 Us_{50} \tag{7}$$

where 0.60 is the mean value of $D_x(Us_{50})^{-1}$ at $Re_d > 100$. Equation (7) is shown as the dashed line in Fig. 5. While Eq. (7) is empirical, it is similar to Eq. (4) by analogy, containing s_{50} instead of s^*, and reflecting velocity-field heterogeneity through U and s_{50} combined.
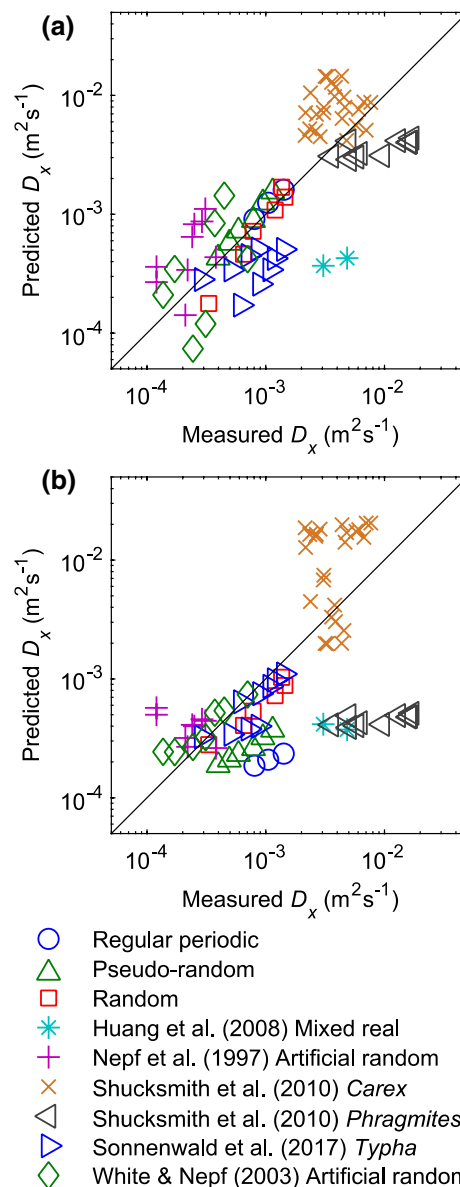

Fig. 6 Predicted D_x for $Re_d > 100$ using **a** Eq. (7) and **b** Eqs. (4) and (5) compared to measured D_x, line is line of equality

Fig. 7 Comparison of RMSE between predicted D_x and measured D_x for $Re_d > 100$ between Eq. (7) and Eqs. (4) and (5), lower values are better
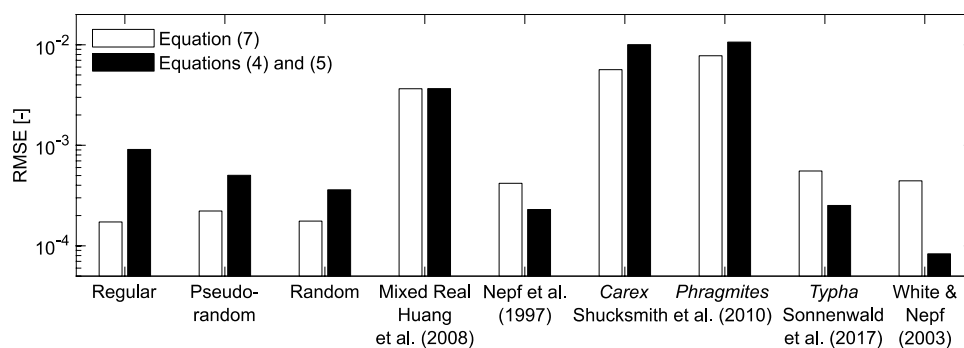

Figure 6a shows predictions of D_x made using Eq. (7) compared to measured values of D_x from the present study as well as from other the experimental studies listed in Table 1. Mean s, estimated from d and ϕ, was used instead of s_{50} for the other studies as s_{50} was not available. As expected from Fig. 5, D_x is accurately predicted for the regular periodic, pseudo-random, and random vegetation configurations. The data from White and Nepf (2003) and Nepf et al. (1997), collected from cylinder arrays, are reasonably predicted. Notably, the Shucksmith et al. (2010) and Sonnenwald et al. (2017) real vegetation are also predicted well.

Figure 6b shows predictions of D_x made using Eqs. (4) and (5) compared to measured values of D_x. Equations (4) and (5) offer a better prediction of D_x for data from Nepf et al. (1997), White and Nepf (2003), and Sonnenwald et al. (2017) than Eq. (7). The vegetation from this study and the vegetation of Shucksmith et al. (2010) are less well predicted. Neither Eq. (7) nor Eqs. (4) and (5) predict the Huang et al. (2008) real vegetation well. Predictions with Eqs. (4) and (5) are biased towards underestimates of D_x. The scatter of predictions from Eq. (7) may be due to the use of an estimated value of s rather than a measured value.

Figure 7 compares RMSE goodness of fit between measured and predicted D_x made using Eq. (7) and measured and predicted D_x made using Eqs. (4) and (5). It shows the overall quality of predictions to be very similar. Equation (7) predicts the correct order of magnitude dispersion coefficient and is a suitable engineering approximation at $\phi < 0.1$. It predicts dispersion coefficient in real vegetation as well or better than Eqs. (4) and (5) in three out of four cases, despite the inherent variability of real vegetation.

Normalisation by median stem spacing, rather than stem diameter, appears to be a useful method of incorporating spatial heterogeneity into non-dimensional longitudinal dispersion coefficient, as it is successful in distinguishing between vegetation arrangements. However, it is worth noting that s_{50}, like d, is still a single length-scale characterisation. Most current theory is based on one such characterisation, while in reality multiple length scales are common, as described in Sonnenwald et al. (2017).

Future work should investigate the suitability of Eq. (7) at higher solid volume fractions and for more types of vegetation. Additional work is also needed to investigate how vegetation is described when calculating dispersion coefficient in complex vegetation arrangements, e.g. with varying stem diameter or stem spacing distributions.

Conclusions

Longitudinal dispersion coefficient (D_x) values obtained from dye tracing in artificial emergent vegetation fitted the expected trend of a linear increase with velocity, but could not be normalised using stem diameter. Stem spacing is suggested here for the first time as the appropriate length-scale normalisation for D_x in vegetation. From this, D_x in vegetation can be modelled by a new simple expression dependent on median stem edge-to-edge spacing. This new model showed reasonable performance when applied to other experimental data, including real vegetation. Although a more complex expression from the literature predicts D_x in vegetation equally well, it has multiple implicit assumptions. The new expression presented here gives robust correct order of magnitude estimates of longitudinal dispersion coefficient in vegetation suitable for engineering purposes.

References

Danish Hydraulic Institute (2009) MIKE 11: a modelling system for rivers and channels. Reference manual. Denmark

Ergun S (1952) Fluid flow through packed columns. Chem Eng Prog 48:89–94

Fischer HB, List JE, Koh CR, Imberger J, Brooks NH (1979) Mixing in inland and coastal waters. Elsevier, Amsterdam

Huang YH, Saiers JE, Harvey JW, Noe GB, Mylon S (2008) Advection, dispersion, and filtration of fine particles within emergent vegetation of the Florida everglades. Water Resour Res 44:W04408

Lightbody AF, Nepf HM (2006) Prediction of velocity profiles and longitudinal dispersion in emergent salt marsh vegetation. Limnol Oceanogr 51(1):218–228

Nepf HM (1999) Drag, turbulence, and diffusion in flow through emergent vegetation. Water Resour Res 35(2):479–489

Nepf HM (2012) Flow and transport in regions with aquatic vegetation. Annu Rev Fluid Mech 44:123–142

Nepf HM, Mugnier C, Zavistoski R (1997) The effects of vegetation on longitudinal dispersion. Estuar Coast Shelf Sci 44(6):675–684

O'Hare MT (2015) Aquatic vegetation—a primer for hydrodynamic specialists. J Hydraul Res 53(6):687–698

Shucksmith J, Boxall J, Guymer I (2010) Effects of emergent and submerged natural vegetation on longitudinal mixing in open channel flow. Water Resour Res 46(4):W04504

Sonnenwald F, Guymer I, Marchant A, Wilson N, Golzar M, Stovin V (2016). Estimating stem-scale mixing coefficients in low velocity flows. In: sustainable hydraulics in the era of global change: proceedings of the 4th IAHR Europe congress. CRC Press

Sonnenwald F, Hart J, West P, Stovin V, Guymer I (2017) Transverse and longitudinal mixing in real emergent vegetation at low velocities. Water Resour Res 53(1):961–978

Sonnenwald F, Stovin V, Guymer I (2018a) Use of drag coefficient to predict dispersion coefficients in emergent vegetation at low velocities. Paper presented at the 12th international symposium on ecohydraulics, Tokyo, Japan

Sonnenwald F, Stovin V, Guymer I (2018b) Estimating drag coefficient for arrays of rigid cylinders representing vegetation. J Hydraul Res. https://doi.org/10.1080/00221686.2018.1494050

Tanino Y (2012) Flow and mass transport in vegetated surface waters. In: Gualtieri C, Mihailovic DT (eds) Fluid mechanics of environmental interfaces, 2nd edn. Taylor & Francis, Abingdon, pp 369–394

Tanino Y, Nepf HM (2008) Lateral dispersion in random cylinder arrays at high Reynolds number. J Fluid Mech 600:339–371

The MathWorks Inc (2018) MATLAB R2018a, Natick, MA

Tinoco RO, Cowen EA (2013) The direct and indirect measurement of boundary stress and drag on individual and complex arrays of elements. Exp Fluids 54(4):1–16

White BL, Nepf HM (2003) Scalar transport in random cylinder arrays at moderate Reynolds number. J Fluid Mech 487:43–79

Woods-Ballard B, Wilson S, Udale-Clarke H, Illman S, Scott T, Ashley R, Kellagher R (2015) The SUDS manual, report C753. CIRIA, London